

A Differential Geometric Approach to Classification

Qinxun Bai

Department of Computer Science, Boston University

QINXUN@CS.BU.EDU

Steven Rosenberg

Department of Mathematics and Statistics, Boston University

SR@MATH.BU.EDU

Stan Sclaroff

Department of Computer Science, Boston University

SCLAROFF@CS.BU.EDU

Abstract

We use differential geometry techniques to study the classification problem to estimate the conditional label probability for learning a plug-in classifier. In particular, we propose a geometric regularization technique to find the optimal hypersurface corresponding to the estimator of η . The regularization term measures the total Riemannian curvature of the hypersurface corresponding to the estimator of η , based on the intuition that overfitting corresponds to fast oscillations and hence large curvature of the estimator. We use gradient flow type methods to move from an initial estimator towards a minimizer of a penalty function that penalizes both the deviation of the hypersurface from the training data and the total curvature of the hypersurface. We establish Bayes consistency for our algorithm under mild initialization assumptions and implement a discrete version of this algorithm. In experiments for binary classification, our implementation compares favorably to several widely used classification methods.

Keywords: Classification, plug-in classifier, regularization methods, mean curvature, geometric flow, Bayes consistency

1. Introduction

We study the classification problem in the probabilistic setting. Given a sample space \mathcal{X} , a label space \mathcal{Y} , and a finite training set of labeled samples $\mathcal{T}_m = \{(\mathbf{x}_i, y_i)\}_{i=1}^m \in (\mathcal{X} \times \mathcal{Y})^m$, where each training sample is generated independently from some underlying distribution P over $\mathcal{X} \times \mathcal{Y}$, our goal is to find a $h_{\mathcal{T}_m} : \mathcal{X} \rightarrow \mathcal{Y}$ such that for any new sample $\mathbf{x} \in \mathcal{X}$, $h_{\mathcal{T}_m}$ predicts its label $\hat{y} = h_{\mathcal{T}_m}(\mathbf{x})$. The performance of $h_{\mathcal{T}_m}$ is measured by the generalization error (risk) $R_P(h_{\mathcal{T}_m}) = \mathbb{E}_P[\mathbb{1}_{h_{\mathcal{T}_m}(\mathbf{x}) \neq y}]$, and the Bayes risk is defined by $R_P^* = \inf_{h: \mathcal{X} \rightarrow \mathcal{Y}} R_P(h)$. For binary classification where $\mathcal{Y} = \{1, -1\}$, the Bayes risk is achieved by the classifier $h^*(\mathbf{x}) = \text{sign}(\eta(\mathbf{x}) - 0.5)$, where $\eta : \mathcal{X} \rightarrow [0, 1]$ is the conditional label probability $\eta(\mathbf{x}) = P(y = 1|\mathbf{x})$. Our method follows the plug-in classification scheme (Audibert and Tsybakov, 2007), i.e. find a nonparametric estimator $f : \mathcal{X} \rightarrow [0, 1]$ of the function η and “plug-in” f to get the plug-in classifier $h_f(\mathbf{x}) = \text{sign}(f(\mathbf{x}) - 0.5)$.

In learning f from training data, our method shares the philosophy of regularization methods (Vapnik, 1998; Schölkopf and Smola) in seeking a balance between a perfect description of the training data and the potential for generalization. As usual, our approach also minimizes a data term and a regularization term to prevent overfitting. The novelty is that we introduce a geometric perspective to formulate the learning process as a hypersurface fitting problem that can be solved by a geometric flow method.

While the empirical risk based probabilistic setting enables interesting asymptotic analysis on the generalization ability and consistency of many regularization methods (Steinwart, 2005; Bousquet and Elisseeff, 2002) and plug-in classifiers (Audibert and Tsybakov, 2007), we feel that there is geometric information, of both a metric and curvature nature, that is not fully captured by this probabilistic framework. A basic observation is that in many real world problems, if the feature space is meaningful, then all samples within a small enough neighborhood of a training sample point should have conditional label probability $\eta(\mathbf{x})$ similar to the training sample. For instance, a small enough perturbation of RGB values at some pixels of a human face image should not change the identity of this image during face recognition. Following this viewpoint, we suggest a geometric perspective that overfitting is related to rapid oscillations of the estimator f of η : if we regard $(\mathbf{x}, f(\mathbf{x}))$ as a hypersurface in $\mathcal{X} \times [0, 1]$, these oscillations can be measured by the total curvature of this hypersurface. In other words, we believe that a reasonable way to generalize from finite training samples to an estimation of η on the whole space \mathcal{X} is to find a hypersurface to fit the training samples such that it is as flat as possible in the Riemannian curvature sense.

In more detail, we use differential geometry terminology to characterize this hypersurface as the graph of a function $f : \mathcal{X} \rightarrow [0, 1]$ defined by $\text{gr}(f) = \{(\mathbf{x}, f(\mathbf{x})) : \mathbf{x} \in \mathcal{X}\}$. For example, for $\eta(\mathbf{x})$, we have $\mathcal{X} \subseteq \mathbb{R}^N$, $\mathcal{Y} = \{-1, 1\}$, $\mathcal{X} \times [0, 1] \subset \mathbb{R}^{N+1}$ with coordinates (x^1, \dots, x^{N+1}) , where $(x^1, \dots, x^N) = \mathbf{x} \in \mathcal{X}$ and $x^{N+1} = \eta(\mathbf{x})$ on $\text{gr}(\eta)$. To make our training point $(\mathbf{x}_i, y_i = \pm 1)$ compatible with these coordinates, we map $(\mathbf{x}_i, y_i = 1)$ to $(\mathbf{x}_i, 1)$ on the hyperplane $x^{N+1} = 1$ and map $(\mathbf{x}_i, y_i = -1)$ to $(\mathbf{x}_i, 0)$ on the hyperplane $x^{N+1} = 0$. The graph of any estimator f is a hypersurface lying between these hyperplanes. We want f to approach the mapped training points while remaining as flat as possible, so we impose a penalty function on the graph of f consisting of a data term and a geometric regularization term. For the data term, we define a distance penalty on $\text{gr}(f)$, which is an L^2 measure of the distance from a graph point to its nearest mapped training point. For the geometric regularization term, we consider an L^2 measure of the curvature of $\text{gr}(f)$. In particular, we adopt the most informative measure, i.e. $\mathcal{C}'(f) = \int_{\text{gr}(f)} |\mathcal{R}_f|^2 \text{dvol}$, where \mathcal{R}_f is the Riemannian curvature tensor of the graph of f , and dvol is the induced volume form, since \mathcal{R}_f is the obstruction to the flatness of the graph, and dvol measures the volume distortion from Lebesgue measure on \mathcal{X} .

Once we have the penalty function (given in §3), consisting of the data term plus the geometric regularization term, defined on the infinite dimensional space $\{f : \mathbb{R}^n \rightarrow [0, 1]\}$, we can explicitly derive the Euler-Lagrange equations describing the critical functions. However, since f is nonparametric, these equations are difficult to solve explicitly, so we adapt gradient flow methods to find an optimal direction, i.e. a vector field on the graph of an initial estimator f that determines an optimal direction to move f . In other words, we can start with a reasonable initial graph, and then flow in the direction that minimizes the penalty. In particular, we choose as our initial graph $f(\mathbf{x}) \equiv \frac{1}{2}$, which is a reasonable choice without any prior information. In theory, in the limit (given infinite time) we will flow to a critical graph, and for generic initial graphs, we expect the infinite time limit to be a local minimum for the penalty function. These gradient flow methods are familiar in finite dimensional Morse theory (Milnor, 1963) and in geometric PDE theory (Audin and Damian, 2014).

To relate our work to statistical learning theory, we show that under some mild assumptions on initialization, our algorithm is Bayes consistent. We also discuss the extension of this method to multi-class problems in §3.4. The main insight is that by simply passing from a hypersurface in \mathbb{R}^{N+1} to a submanifold of \mathbb{R}^{N+K} , we can treat the K -class problem with the same techniques through training the graph of a single function $f : \mathbb{R}^N \rightarrow \mathbb{R}^K$, as opposed to the $O(K)$ classi-

fiers (or $O(\log_2 K)$) classifiers via binary coding [Varshney and Willsky, 2010](#)) in the usual K -class techniques, which we feel is a significant advance in this subject. Our implementation for binary classification compares favorably to widely used classification methods on benchmark datasets from the UCI repository.

In summary, our contributions are:

1. We propose a geometric setup for classification, which estimates the conditional label probability η by fitting a hypersurface corresponding to the estimator of η .
2. We propose a geometric regularization term using the total Riemannian curvature of the corresponding hypersurface as a measure of the oscillation of the estimator of η .
3. We adapt a geometric flow method to solve the proposed variational formula and show Bayes consistency for our algorithm under some mild initialization assumptions.

A summary of notation used in the paper and proofs of main results are given in the appendices.

2. Related Work

Our method differs from most existing regularization methods in two aspects. Firstly, it is based on plug-in classifier design ([Audibert and Tsybakov, 2007](#)), and not the standard empirical risk minimization (ERM) scheme. Secondly, it seeks an optimal nonparametric estimator of the conditional label probability η through a novel geometric setup: by mapping each training pair (x_i, y_i) to a data point in the space $\mathcal{X} \times [0, 1]$, supervised learning for binary classification is converted to a procedure of finding the optimal graph of a function embedded in $\mathcal{X} \times \mathbb{R}$ that balances between fitting the mapped training data and minimizing the total curvature of the graph. The same procedure also generalizes naturally to multi-class problems, which enables training a single graph to do multi-class classification, in contrast with the traditional one-versus-all training process. To the best of our knowledge, such a geometric framework for binary and multi-class classification does not exist in the machine learning literature.

Regarding the two terms of our penalty function, the data term is most closely related to the nearest neighbor classifier ([Cover and Hart, 1967](#); [Devroye et al., 1996](#)), though learning the nearest neighbor classifier is not formulated as a minimization problem. For the regularization term, there are existent methods that introduce geometric regularization terms to measure the “smoothness” of the decision boundary ([Cai and Sowmya, 2007](#); [Varshney and Willsky, 2010](#); [Lin et al., 2012](#)); the most related work [Varshney and Willsky \(2010\)](#) uses the volume as the measure of smoothness, but still follows the regularized ERM scheme, and thus is different from our setup. Regarding the geometric term itself, our method differs from [Varshney and Willsky \(2010\)](#) in two ways: firstly, it measures the flatness of the graph of the estimator of η in $\mathcal{X} \times [0, 1]$, which encodes more geometric information than the [Varshney and Willsky \(2010\)](#) measurement of the volume of the decision boundary in \mathcal{X} ; secondly, we introduce the total Riemannian curvature as the measurement of flatness and derive a gradient vector field formula for the general manifold embedding situation, given in Theorem 1, which is novel to machine learning.

Our training procedure of finding the optimal graph of a function is, in a general sense, also related to the manifold learning problem ([Tenenbaum et al., 2000](#); [Roweis and Saul, 2000](#); [Belkin and Niyogi, 2003](#); [Donoho and Grimes, 2003](#); [Zhang and Zha, 2005](#); [Lin and Zha, 2008](#)). The most closely related work is [Donoho and Grimes \(2003\)](#), which also tries to find a flat submanifold

of Euclidean space that contains a dataset. Again, there are key differences. Since their goal is dimensionality reduction, their manifold has high codimension, while our graph is a hypersurface. More importantly, we do not assume that the graph of our function is a flat hypersurface, and we attempt to flow to a function whose graph is as flat as possible. In this regard, our work is related to a large body of literature on gradient flow/Morse theory in finite dimensions (Milnor, 1963) and in infinite dimensions (Audin and Damian, 2014), and on mean curvature flow, see Chen et al. (1999); Mantegazza (2011) and the references therein.

3. The Differential Geometric Method

Our regularized penalty function \mathcal{P} consists of two terms, the first is a data term measured by a distance function that penalizes the deviation of perfectly fitting the mapped training samples, and the second is a geometric term that penalizes the total Riemannian curvature of the classifier.

As explained in §1, we want to find the (or a) best estimator $f : \mathcal{X} \rightarrow [0, 1]$ of η on a compact set $\mathcal{X} \subset \mathbb{R}^N$ given a set of training data $\mathcal{T}_m = \{(x_i, y_i)\}_{i=1}^m$. We think of \mathcal{X} as large enough so that the training data actually is sampled well inside \mathcal{X} . This allows us to treat \mathcal{X} as a closed manifold in our gradient calculations, so that boundary effects can be ignored.

To be more precise, we consider the Fréchet manifold/vector space \mathcal{M} of maps from \mathcal{X} to $(0 - \epsilon, 1 + \epsilon)$ for some positive ϵ . The Fréchet topology is given as follows: a basis of the topology at a function $f \in \mathcal{M}$ consists of all functions f' with $\sup_{\alpha_k} \|\partial_{\alpha_k}(f' - f)\|_{\infty} < \delta_k$ for all $k \in \mathbb{Z}_{\geq 0}$, for choices of $\delta_k > 0$, where ∂_{α_k} ranges over all partial derivatives of order k . The ϵ factor is inserted to assure that \mathcal{M} is an open subset of $\text{Maps}(\mathcal{X}, \mathbb{R})$ and hence an infinite dimensional manifold without boundary. The penalty function $\mathcal{P} : \mathcal{M} \rightarrow \mathbb{R}$ should be Fréchet smooth or at least differentiable, so that the gradient method can be applied.

To explain the gradient method, we consider the tangent space $T_f\mathcal{M}$ at f . Since \mathcal{M} is a subset of the vector space $\text{Maps}(\mathcal{X}, \mathbb{R})$, we can canonically identify $T_f\mathcal{M}$ with \mathcal{M} . We take the L^2 metric on each tangent space $T_f\mathcal{M}$: $\langle \phi_1, \phi_2 \rangle := \int_{\mathcal{X}} \phi_1(x)\phi_2(x)d\text{vol}_x$, with $\phi_i \in \mathcal{M}$ and $d\text{vol}_x$ the volume form of the induced Riemannian metric on the graph of f . (Strictly speaking, the volume form is pulled back to \mathcal{X} by f , usually denoted $f^*d\text{vol}$.) We could alternatively use Lebesgue measure on \mathcal{X} in this integral, but $d\text{vol}$ generalizes to the case where \mathcal{X} is itself a manifold.

Since \mathcal{P} is smooth, its differential $d\mathcal{P}_f : T_f\mathcal{M} \rightarrow \mathbb{R}$ is defined for each f . Since $d\mathcal{P}_f$ is linear and since smooth functions are dense in L^2 , there is a unique tangent vector $\nabla\mathcal{P}_f \in T_f\mathcal{M}$ such that $d\mathcal{P}_f(\phi) = \langle \nabla\mathcal{P}_f, \phi \rangle$ for all $\phi \in T_f\mathcal{M}$. The gradient vector field $\nabla\mathcal{P}$ is smooth in f . As in finite dimensions, $\nabla\mathcal{P}_f$ points in the direction of steepest growth of \mathcal{P} at f , and given an initial point $f \in \mathcal{M}$, the associated (negative) gradient flow line through f is the solution of $\frac{df_t}{dt} = -\nabla\mathcal{P}_{f_t}$, $f_0 = f$, for $f_t \in \mathcal{M}$ and $t \geq 0$. \mathcal{M} is a tame Fréchet space in the sense of Hamilton (1982), so the existence of gradient lines is plausible. As in finite dimensions (Milnor, 1963), a generic initial point flows to a local minimum of \mathcal{P} as $t \rightarrow \infty$. For $t \gg 0$, the (L^2 or pointwise) length of the gradient vector along the flow goes to zero, and we could stop the flow when this length is below a specified cutoff.

We will always choose $f = f_0$ to be the “neutral” choice $f(x) \equiv \frac{1}{2}$.

We write $\mathcal{P} = \mathcal{P}_D + \mathcal{P}_G$, where \mathcal{P}_D is the distance penalty (data term) and \mathcal{P}_G is the geometric penalty (regularization term).

3.1. The distance penalty \mathcal{P}_D

The most natural geometric distance penalty term is the total L^2 distance error:

$$\mathcal{P}_D(f) = \int_{\mathcal{X}} d^2((\mathbf{x}, f(\mathbf{x})), (\tilde{\mathbf{x}}, \tilde{x}^{N+1})) d\text{vol}(\mathbf{x}),$$

where d is the Euclidean distance in \mathbb{R}^{N+1} and $\tilde{\mathbf{x}} \in \mathcal{X}$ is the (not necessarily unique) closest point in the training data to \mathbf{x} and \tilde{x}^{N+1} is the $N + 1$ -st component value (either 1 or 0) associated to $(\tilde{\mathbf{x}}, \tilde{y})$, as in §1. In particular, \mathcal{P}_D is invariant under diffeomorphisms of \mathcal{X} .

Under the assumption that each point has a unique nearest neighbor, one can show that

$$\begin{aligned} \nabla(\mathcal{P}_D)_f(\mathbf{x}, f(\mathbf{x})) &= 2((\mathbf{x}, f(\mathbf{x})) - ((\tilde{\mathbf{x}}, \tilde{x}^{N+1}))) - d^2((\mathbf{x}, f(\mathbf{x})), (\tilde{\mathbf{x}}, \tilde{x}^{N+1})) \text{Tr II} \\ &\quad - 2 \sum_{r,l=1}^k \sum_{j=1}^N g^{rl}((\mathbf{x}, f(\mathbf{x}))^j - (\tilde{\mathbf{x}}, \tilde{x}^{N+1})^j) \frac{\partial f^j}{\partial x^l} \Big|_{\mathbf{x}} \partial_r. \end{aligned} \quad (1)$$

Here (g_{rl}) is the Riemannian metric matrix induced on the graph of f from the Euclidean metric on \mathbb{R}^{N+1} , (g^{rl}) is its inverse matrix, and Tr II is the trace of the second fundamental form (see Appendix A). For points with multiple nearest neighbors, we could *e.g.* form the average of the distances squared to the set of nearest neighbors.

This flow is fine for more general data approximation problems, but has several difficulties in the graph/classifier case. First, it is not clear that the flow f_t is the graph of a function for all t . In fact, Tr II is always normal to the graph of f , and the first and third terms on the righthand side of (1) form the projection of $2((\mathbf{x}, f(\mathbf{x})) - (\tilde{\mathbf{x}}, \tilde{x}^{N+1}))$ into the normal direction. Thus, the flow vectors are always normal to the graph. Since the flow is not necessarily in the $N + 1$ -coordinate direction in \mathbb{R}^{N+1} , it is unclear that the flow of a graph remains a graph of a function.

We can force the gradient vector to point in the $N + 1$ -coordinate direction by modifying the distance penalty term to the following risk, still denoted $\mathcal{P}_D(f)$ or $R_{D,\mathcal{T}_m,k}(f)$,

$$\mathcal{P}_D(f) = R_{D,\mathcal{T}_m,k}(f) = \int_{\mathcal{X}} d^2 \left(f(\mathbf{x}), \frac{1}{k} \sum_{i=1}^k \tilde{x}_i^{N+1} \right) d\mathbf{x},$$

where k is fixed, \tilde{x}_i^{N+1} is the $(N + 1)$ -st component value associated to the i^{th} nearest neighbor in \mathcal{T}_m to \mathbf{x} , and $d\mathbf{x}$ is Lebesgue measure. This is an L^2 version of a k -nearest neighbor penalty. The gradient vector field is

$$\nabla(R_{D,\mathcal{T}_m,k})_f(\mathbf{x}, f(\mathbf{x})) = \frac{2}{k} \sum_{i=1}^k (\mathbf{0}, f(\mathbf{x}) - \tilde{x}_i^{N+1}).$$

However, $\nabla(R_{D,\mathcal{T}_m,k})_f$ is discontinuous on the set \mathcal{D} of points \mathbf{x} such that \mathbf{x} has equidistant training points among its k nearest neighbors. \mathcal{D} is the union of $(N - 1)$ -dimensional hyperplanes in \mathcal{X} , so \mathcal{D} has measure zero. Such points will necessarily exist unless the $(N + 1)$ -st component values of the mapped training points are always 1 or always 0. To rectify this, we can smooth out $\nabla(R_{D,\mathcal{T}_m,k})_f$ to a vector field

$$V_{D,f,\phi} = \frac{2\phi(\mathbf{x})}{k} \sum_{i=1}^k (\mathbf{0}, f(\mathbf{x}) - \tilde{x}_i^{N+1}). \quad (2)$$

Here $\phi(x)$ is a smooth function close to the singular function $\delta_{\mathcal{D}}$, which has $\delta_{\mathcal{D}}(x) = 0$ for $x \in \mathcal{D}$ and $\delta_{\mathcal{D}}(x) = 1$ for $x \notin \mathcal{D}$. Outside any open neighborhood of \mathcal{D} , $\nabla R_{D, \tau_m, k} = V_{D, f, \phi}$ for ϕ close enough to $\delta_{\mathcal{D}}$.

3.2. The geometric penalty \mathcal{P}_G

As discussed in §1, we wish to penalize graphs for excessive curvature. Very sensitive measures are given by the L^2 norm of the length of the Riemann curvature tensor: $\int_{\mathcal{X}} |\mathcal{R}_f|^2 f^* \text{dvol}$ or the L_∞ norm $\|\mathcal{R}_f\|_\infty = \sup_{x \in \mathcal{X}} |\mathcal{R}_{(x, f(x))}|$. Minimization of Riemannian curvature corresponds to finding the graph with the least distortion of lengths and angles, i.e., minimizing $|d_f((x_1, f(x_1)), (x_2, f(x_2))) - d_{\mathbb{R}^N}(\phi^{-1}(x_1, f(x_1)), \phi^{-1}(x_2, f(x_2)))|$, where d_f is the geodesic distance on the graph of f , $d_{\mathbb{R}^N}$ is the standard Euclidean distance, and ϕ ranges over all diffeomorphisms from \mathbb{R}^N to $\text{gr}(f)$. This is similar to the approach in [Donoho and Grimes \(2003\)](#).

We choose as curvature penalty function

$$\mathcal{P}_G(f) = \int_{\mathcal{X}} |\mathcal{R}_f|^2 f^* \text{dvol} = \int_{\text{gr}(f)} |\mathcal{R}_f|^2 \text{dvol} = \int_{\text{gr}(f)} \mathcal{R}_{ijkl} \mathcal{R}^{ijkl} \text{dvol}, \quad (3)$$

where $\mathcal{R} = R_{ijkl} dx^i \otimes dx^j \otimes dx^k \otimes dx^l$ is the Riemann curvature tensor for the Riemannian metric on $\text{gr}(f)$ induced from the Euclidean metric on \mathbb{R}^{N+1} , and dvol is the induced volume form. We always use summation convention on repeated indices. As with the original \mathcal{P}_D , this penalty term has the desirable property of being invariant under diffeomorphisms/reparametrizations of \mathcal{X} , while, e.g., $\int_{\mathcal{X}} |\mathcal{R}_f|^2 dx$ is not.

We have the following theorem for the gradient vector field of \mathcal{P}_G . In this theorem, we work in a more general setup, with \mathcal{X} replaced by a manifold M . (However, for simplicity we assume that M is compact without boundary; see [Bai et al. \(2015\)](#) for the boundary terms in the case of a manifold with boundary and for the proof of the theorem below.)

Theorem 1 *Let $\phi = (\phi^1, \dots, \phi^{N+1}) : M \rightarrow \mathbb{R}^{N+1}$ be an embedding. The gradient vector field for \mathcal{P}_G at ϕ is the \mathbb{R}^{N+1} -valued vector field $Z = (Z^1, \dots, Z^{N+1})$ defined on $\phi(M)$ with α component*

$$\begin{aligned} Z^\alpha = & 6 \frac{1}{\sqrt{\det(g)}} \partial_r \left(\sqrt{\det(g)} R_{jkl}^r \phi_i^\alpha R^{ijkl} \right) \\ & + 2 \frac{1}{\sqrt{\det(g)}} \partial_z \left(\left[\frac{1}{\sqrt{\det(g)}} ([\phi_{lj}^\alpha - \phi_r^\alpha \Gamma_{lj}^r] \partial_m (R^{mjz} \sqrt{\det(g)})) \right. \right. \\ & + (\phi_{ljm}^\alpha - \phi_{rm}^\alpha \Gamma_{lj}^r - \phi_r^\alpha \partial_m (\Gamma_{lj}^r)) R^{mjz} \\ & \left. \left. + \Gamma_{nk}^z [\phi_{lj}^\alpha - \phi_r^\alpha \Gamma_{lj}^r] R^{njl k} \right] \sqrt{\det(g)} \right) \\ & - |\mathcal{R}|^2 (\text{Tr II})^\alpha - 2 \langle \nabla \mathcal{R}, \mathcal{R} \rangle^{\sharp, \alpha}. \end{aligned}$$

Here (i) $\det(g)$ is the determinant of the induced metric tensor in local coordinates on $\phi(M)$ coming from local coordinates on M composed with ϕ , (ii) $\phi_i^\alpha, \phi_{rm}^\alpha$, etc. denote partial derivatives of ϕ^α in these local coordinates and ∂_z is the z^{th} partial derivative, (iii) Γ_{lj}^r are the Christoffel symbols of the induced metric on $\phi(M)$, (iv) ∇R is the covariant derivative of R , (v) $\langle \nabla \mathcal{R}, \mathcal{R} \rangle$ is the one-form on \mathcal{M} given by contracting $\nabla \mathcal{R}$ with \mathcal{R} , (vi) $\langle \nabla \mathcal{R}, \mathcal{R} \rangle^{\sharp, \alpha}$ is the α component of the

dual vector field on M . In the graph case, the embedding ϕ associated to the function $f : \mathcal{X} \rightarrow \mathbb{R}$ is the graph of f : $\phi(\mathbf{x}) = (\mathbf{x}, f(\mathbf{x}))$.

This formula is complicated, but the main point is that embeddings with minimal/vanishing geometric penalty are flat, i.e. the embedding admits distortion-free coordinate maps to \mathbb{R}^N . In contrast, for a simpler penalty function $\int_{\text{gr}(f)} \text{dvol}$, minima of this functional are just that: embeddings with (locally) minimal volume. While the geometric penalty is more informative, a careful count shows that the vector field Z involves four derivatives of the embedding ϕ , while the variation vector field for $\int_{\text{gr}(f)} \text{dvol}$ only involves two derivatives. It seems difficult to control errors in numerical computations of the gradient flow for Z . This is really the only reason to adopt the less refined volume penalty term.

As a result, for numerical concerns we work in our implementation with $\mathcal{P}_G := \int_{\text{gr}(f)} \text{dvol}$, the volume of the graph of f . This involves a subtle shift from an intrinsic quantity $\| |\mathcal{R}_f| \|_\infty$ (i.e. a quantity independent of isometries of the graph of f) to an extrinsic quantity (i.e. a quantity that is independent only under isometries of all of \mathbb{R}^{N+1}). We have $\nabla \mathcal{P}_G = \text{Tr II}$ on the space of all embeddings of X in \mathbb{R}^{N+1} (Lawson, 1980). If we restrict to the submanifold of graphs of $f \in \text{Maps}(\mathcal{X}, \mathbb{R})$, then $\nabla \mathcal{P}_G$ must point in the e_{N+1} direction, and it is easy to calculate that the gradient is

$$V_{G,f} = (\text{Tr II} \cdot e_{N+1})e_{N+1}. \quad (4)$$

An explicit formula for Tr II for graphs $\text{gr}(f)$ is given by Jagy (1991)

$$\text{Tr II} = \frac{1}{N\sqrt{1+|\nabla f|^2}} \sum_{i,j=1}^N \left(\delta_{ij} - \frac{f_i f_j}{1+|\nabla f|^2} \right) f_{ij},$$

where f_i, f_{ij} denote partial derivatives of f .

3.3. Total vector field

The total vector field at $f \in \mathcal{M}$ is by definition

$$\begin{aligned} V_{\text{tot}, \lambda, m, f, \phi} &= V_{D, f, \phi} + \lambda V_{G, f} \\ &= \frac{2\phi(\mathbf{x})}{k} \sum_{i=1}^k (\mathbf{0}, f(\mathbf{x}) - \tilde{x}_i^{N+1}) + \lambda (\text{Tr II} \cdot e_{N+1})e_{N+1}. \end{aligned} \quad (5)$$

where λ is the trade-off parameter of the two terms \mathcal{P}_D and \mathcal{P}_G .

3.4. Extension to multi-class classification

For the multi-class classification problem, given a compact set $\mathcal{X} \subset \mathbb{R}^N$, $\mathcal{Y} = \{1, 2, \dots, K\}$ and a set of training data $\mathcal{T} = \{(\mathbf{x}_i, y_i)\}_{i=1}^m$ with $\mathbf{x}_i \in \mathcal{X}, y_i \in \mathcal{Y}$, we have $\mathcal{X} \times [0, 1]^K \subset \mathbb{R}^{N+K}$ with coordinates (x^1, \dots, x^{N+K}) , where $(x^1, \dots, x^N) \in \mathcal{X}$ in general and $x^{N+j} = P(y = j | \mathbf{x})$ for the j^{th} conditional label probability. Now all training points $(\mathbf{x}_i, y_i = j)$ are mapped as in the binary case to lie on the N dimensional affine space $(x^{N+1}, \dots, x^{N+j}, \dots, x^{N+K}) = (0, \dots, 1, \dots, 0)$. We can modify the binary formulation to search for the best multi-variate function $f : \mathcal{X} \rightarrow [0, 1]^K$, where $f = (f^1, \dots, f^K)$ with $f^j : \mathcal{X} \rightarrow [0, 1]$ as an estimator of $P(y = j | \mathbf{x})$, and the graph of f is the subset of \mathbb{R}^{N+K} given by $\text{gr}(f) = (\mathbf{x}, f^1(\mathbf{x}), \dots, f^K(\mathbf{x}))$. As in the binary case, we

should start with the N dimensional affine space $\{x^{N+1} = \dots = x^{N+K} = \frac{1}{K}\}$; this is the graph of $f_0 \equiv \frac{1}{K}$. After these modifications, the form of the penalty function for the multi-class case is the same as in the binary case, which can be treated by the same gradient flow strategy.

We compute the gradient vector field which gives the direction of flow at any time $t > 0$. We keep the same distance penalty function and volume penalty function. In particular, the vector field for the distance penalty function carries directly over from the case $K = 1$.

We now verify that there is a computable formula for the volume penalty gradient vector field

$$\text{Tr II} = P^\nu \nabla_{e_i}^{\mathbb{R}^{N+K}} e_i, \quad (6)$$

where $\{e_i\}$ is an orthonormal frame of $\text{gr}(f)$, $\nabla_X^{\mathbb{R}^{N+K}} Y = D_X Y$ is the trivial connection on \mathbb{R}^{N+K} ($D_X Y$ is the directional derivative of the components of Y in the direction X), and P^ν is orthogonal projection into the normal bundle to the graph. Recall that we use summation convention on i . As explained in the proof, Tr II is explicitly computable from f .

Theorem 2 *Let $P^T \mathbf{v} = \sum_{i=1}^N (\mathbf{v} \cdot e_i) e_i$ be the orthogonal projection of \mathbb{R}^{N+K} to the tangent space at a point in $\text{gr}(f)$. Then there are explicit functions $h_i^s, g_i^r : \mathbb{R}^N \rightarrow \mathbb{R}$ such that*

Tr II

$$= (\text{I} - P^T) \left(\sum_{j=1}^N h_i^j \frac{\partial h_i^1}{\partial x^j} + \sum_{l=N+1}^{N+K} \left(\sum_{r=1}^N h_i^r \frac{\partial f^l}{\partial x^r} \right) \frac{\partial h_i^1}{\partial x^l}, \dots, \sum_{j=1}^N h_i^j \frac{\partial g_i^K}{\partial x^j} + \sum_{l=N+1}^{N+K} \left(\sum_{r=1}^N h_i^r \frac{\partial f^l}{\partial x^r} \right) \frac{\partial g_i^K}{\partial x^l} \right).$$

Proof A basis of the tangent space of $\text{gr}(f)$ is given by $\{(0, \dots, \overset{i}{1}, \dots, 0, f_i^1, \dots, f_i^K)\}$, with $f_i^r = \partial f^r / \partial x^i$. Applying Gram-Schmidt gives $\{e_i\}$, which are of the form

$$e_i = (h_i^1, \dots, h_i^N, g_i^1, \dots, g_i^K) \quad (7)$$

for some explicit functions $h_i^s, g_i^r : \mathbb{R}^N \rightarrow \mathbb{R}$. All tangent vectors to $\text{gr}(f)$ are of the form $(\mathbf{v}, f_* \mathbf{v})$ for some $\mathbf{v} \in \mathbb{R}^N$, so $e_i = (\mathbf{v}_i, f_*(\mathbf{v}_i))$ with $\mathbf{v}_i = (h_i^1, \dots, h_i^N)$. At a point $(\mathbf{x}_0, f(\mathbf{x}_0))$ on the graph, we have $D_{e_i} e_i = \frac{d}{dt} \big|_{t=0} e_i(\gamma(t))$, where $\gamma(0) = (\mathbf{x}_0, f(\mathbf{x}_0))$, $\dot{\gamma}(0) = e_i$. We can take $\gamma(t) = (\mathbf{x}_0 + t\mathbf{v}_i, f(\mathbf{x}_0 + t\mathbf{v}_i))$, which implies

$$\nabla_{e_i}^{\mathbb{R}^{N+K}} e_i \quad (8)$$

$$\begin{aligned} &= D_{e_i} e_i = D_{(\mathbf{v}_i, f_*(\mathbf{v}_i))} e_i = \frac{d}{dt} \bigg|_{t=0} (h_i^1(\mathbf{x}_0 + t\mathbf{v}_i), f(\mathbf{x}_0 + t\mathbf{v}_i), \dots, g_i^K(\mathbf{x}_0 + t\mathbf{v}_i), f(\mathbf{x}_0 + t\mathbf{v}_i)) \\ &= \left(\sum_{j=1}^N h_i^j \frac{\partial h_i^1}{\partial x^j} + \sum_{l=N+1}^{N+K} \left(\sum_{r=1}^N h_i^r \frac{\partial f^l}{\partial x^r} \right) \frac{\partial h_i^1}{\partial x^l}, \dots, \sum_{j=1}^N h_i^j \frac{\partial g_i^K}{\partial x^j} + \sum_{l=N+1}^{N+K} \left(\sum_{r=1}^N h_i^r \frac{\partial f^l}{\partial x^r} \right) \frac{\partial g_i^K}{\partial x^l} \right) \end{aligned}$$

We have $P^\nu = \text{I} - P^T$. Combining this with (6), (7), (8) gives an explicit expression for the volume penalty gradient vector:

$-\text{Tr II}$

$$= -(\text{I} - P^T) \left(\sum_{j=1}^N h_i^j \frac{\partial h_i^1}{\partial x^j} + \sum_{l=N+1}^{N+K} \left(\sum_{r=1}^N h_i^r \frac{\partial f^l}{\partial x^r} \right) \frac{\partial h_i^1}{\partial x^l}, \dots, \sum_{j=1}^N h_i^j \frac{\partial g_i^K}{\partial x^j} + \sum_{l=N+1}^{N+K} \left(\sum_{r=1}^N h_i^r \frac{\partial f^l}{\partial x^r} \right) \frac{\partial g_i^K}{\partial x^l} \right).$$



For classification, given an input $x \in \mathcal{X}$, we predict its label y using the trained f as follows:

$$y = \operatorname{argmax}_{j \in \{1, 2, \dots, K\}} f^j(x)$$

4. Consistency Analysis

For a training set \mathcal{T}_m , we let $f_{\mathcal{T}_m}$ be the estimator of the conditional label probability η given by our approach. We denote the generalization risk of the corresponding plug-in classifier $h_{f_{\mathcal{T}_m}}$ by $R_P(f_{\mathcal{T}_m})$. Our algorithm is Bayes consistent if $\lim_{m \rightarrow \infty} R_P(f_{\mathcal{T}_m}) = R_P^*$ holds in probability for all distributions P on $\mathcal{X} \times \mathcal{Y}$. Usually, gradient flow methods are applied to convex functionals, so that a flow line approaches the unique global minimum, where we always assume that an actual minimum lies in the function class considered. In finite dimensional space, a penalty function \mathcal{P} can be perturbed to have nondegenerate critical points, in which case a generic starting function flows to a local minimum; in infinite dimensions, the same generic behavior is expected to hold.

Because our functionals are not convex, and because we are strictly speaking not working with gradient vector fields, we can only hope to prove Bayes consistency for the set of initial estimator in the stable manifold of a stable fixed point (or sink) of the vector field (Guckenheimer and Worfolk, 1993). Recall that a stable fixed point f_0 has a maximal open neighborhood, the stable manifold \mathcal{S}_{f_0} , on which flow lines tend towards f_0 . For the manifold $\mathcal{M} = \operatorname{Maps}(\mathcal{X}, (0, 1))$, the stable manifold for a stable critical point of the vector field $V_{tot, \lambda, m, f, \phi}$ is infinite dimensional.

The proof of Bayes consistency follows these steps:

Step 1: $\lim_{\lambda \rightarrow 0} R_{D, P, \lambda}^* = 0$.

Step 2: $\lim_{n \rightarrow \infty} R_{D, P}(f_n) = 0 \Rightarrow \lim_{n \rightarrow \infty} R_P(f_n) = R_P^*$.

Step 3: For all $f \in \operatorname{Maps}(\mathcal{X}, (0, 1))$, $|R_{D, \mathcal{T}_m}(f) - R_{D, P}(f)| \xrightarrow{m \rightarrow \infty} 0$ in probability.

For the proofs, see Appendix C. Given these steps, we have:

Theorem 3 (Bayes Consistency) *Let m be the size of the training data set. Let $f_{1, \lambda, m} \in \mathcal{S}_{f_{D, \mathcal{T}_m, \lambda}}$, the stable manifold for the global minimum $f_{D, \mathcal{T}_m, \lambda}$ for $R_{D, \mathcal{T}_m, \lambda}^\Omega$, and let $f_{n, \lambda, m, \phi}$ be a sequence of functions on the flow line of $V_{tot, \lambda, m, f, \phi}$ starting with $f_{1, \lambda, m}$ with $t_n \rightarrow \infty$ as $n \rightarrow \infty$. Then $R_P(f_{n, \lambda, m, \phi}) \xrightarrow[\lambda \rightarrow 0, \phi \rightarrow \delta_D]{m, n \rightarrow \infty} R_P^*$ in probability for all distributions P on $\mathcal{X} \times \mathcal{Y}$, if $k/m \rightarrow 0$ as $m \rightarrow \infty$.*

Proof In the notation of Appendix A, if $f_{D, \mathcal{T}_m, \lambda}$ is a global minimum for $R_{D, \mathcal{T}_m, \lambda}^\Omega$, then outside of \mathcal{D} , $f_{D, \mathcal{T}_m, \lambda}$ is the limit of critical points for the negative flow of $V_{tot, \lambda, m, f, \phi}$ as $\phi \rightarrow \delta_D$. To see this, fix an ϵ_i neighborhood \mathcal{D}_{ϵ_i} of \mathcal{D} . For a sequence $\phi_j \rightarrow \delta_D$, $V_{tot, \lambda, m, f, \phi_j}$ is independent of $j \geq j(\epsilon_i)$ on $\mathcal{X} \setminus \mathcal{D}_{\epsilon_i}$, so we find a function f_i , a critical point of $V_{tot, \lambda, m, f, \phi_{j(\epsilon_i)}}$, equal to $f_{D, \mathcal{T}_m, \lambda}$ on $\mathcal{X} \setminus \mathcal{D}_{\epsilon_i}$. Since any $x \notin \mathcal{D}$ lies outside some \mathcal{D}_{ϵ_i} , the sequence f_i converges at x if we let $\epsilon_i \rightarrow 0$. Thus we can ignore the choice of ϕ in our proof, and drop ϕ from the notation.

For our algorithm, for fixed λ, m , we have as above $\lim_{n \rightarrow \infty} f_{n, \lambda, m} = f_{D, \mathcal{T}_m, \lambda}$, i.e.,

$$\lim_{n \rightarrow \infty} R_{D, \mathcal{T}_m, \lambda}^\Omega(f_{n, \lambda, m}) = R_{D, \mathcal{T}_m, \lambda}^\Omega(f_{D, \mathcal{T}_m, \lambda}),$$

for $f_1 \in \mathcal{S}_{f_D, \mathcal{T}_m, \lambda}$. By Step 2, it suffices to show $R_{D,P}(f_{D, \mathcal{T}_m, \lambda}) \xrightarrow[\lambda \rightarrow 0]{m \rightarrow \infty} 0$. In probability, we have $\forall \delta > 0, \exists m > 0$ such that

$$\begin{aligned}
 & R_{D,P}(f_{D, \mathcal{T}_m, \lambda}) \\
 & \leq R_{D,P}(f_{D, \mathcal{T}_m, \lambda}) + \lambda \Omega(f_{D, \mathcal{T}_m, \lambda}) \leq R_{D, \mathcal{T}_m}(f_{D, \mathcal{T}_m, \lambda}) + \lambda \Omega(f_{D, \mathcal{T}_m, \lambda}) + \frac{\delta}{3} \quad (\text{Step 3}) \\
 & = R_{D, \mathcal{T}_m, \lambda}^\Omega(f_{D, \mathcal{T}_m, \lambda}) + \frac{\delta}{3} \leq R_{D, \mathcal{T}_m, \lambda}^\Omega(f_{D, P, \lambda}) + \frac{\delta}{3} \quad (\text{minimality of } f_{D, \mathcal{T}_m, \lambda}) \\
 & = R_{D, \mathcal{T}_m}(f_{D, P, \lambda}) + \lambda \Omega(\eta) + \frac{\delta}{3} \leq R_{D,P}(f_{D, P, \lambda}) + \lambda \Omega(f_{D, P, \lambda}) + \frac{2\delta}{3} \quad (\text{Step 3}) \\
 & = R_{D, P, \lambda}^\Omega(f_{D, P, \lambda}) + \frac{2\delta}{3} = R_{D, P, \lambda}^* + \frac{2\delta}{3} \\
 & \leq \delta, \quad (\text{Step 1})
 \end{aligned}$$

for λ close to zero. Since $R_{D,P}(f_{D, \mathcal{T}_m, \lambda}) \geq 0$, we are done. \blacksquare

5. Implementation

5.1. Technicalities

To successfully implement our geometric approach on machine learning tasks, we must treat several critical technicalities.

Representation of the graph of f

While the theory in §3 treats \mathcal{X} , the domain of f , as a continuous space, for practical computations we have to use either a grid representation or a parametric representation (such as radial basis functions (RBFs)) for f ; similar issues occur in Osher and Sethian (1988); Gelas et al. (2007) for level set functions. Our initial attempt with RBFs suggests that they are insufficient to encode the geometric information for the whole graph of f , although there may be more promising parametric representations. As a result, we implement a grid representation. In particular, we initialize the domain of f as a d^N uniform grid, *i.e.*, for each dimension of the input space, we uniformly sample d points, and f is approximated by its values on the grid point set $\{\hat{x}_1, \hat{x}_2, \dots, \hat{x}_{d^N}\}$. In this representation, the computation of the vector field (5) involves computing second derivatives of f at grid points, which is treated by standard finite difference methods. The grid representation seems unsuitable for the more informative geometric term (3), given the numerical error in approximating fourth derivatives of f .

Boundary effect and size of initial domain

As mentioned in §3.2, although our domain \mathcal{X} presumably has a nontrivial boundary, our current computation of the vector field $V_{tot, \lambda, m, f, \phi}$ does not include any boundary terms. If we expand the domain of f to a large open set $\mathcal{X}' \subset \mathbb{R}^N$ with the training data contained in the relatively small set $\mathcal{X} \subset \mathcal{X}'$, then we expect the flow of f to be negligible near the boundary and hence still concentrated on \mathcal{X} . Therefore, expanding the domain conjecturally should have the effect of imposing boundary conditions which force the boundary terms to vanish. For implementation, we first normalize each dimension of the input feature to a fixed interval, and then choose a grid larger than the feature domain. Of course, as the size of the grid region is increased, the computation cost increases. Thus, there is an inevitable trade-off between computational concerns and boundary

effect issues. In the experiments reported here, we found that choosing the grid region 1.2 times as large as the normalized interval size for the input domain eliminates boundary effects for binary classification.

A summary of the algorithm is given in Algorithm 1. For more information on implementation details and hyper-parameter settings, see Appendix C.

Algorithm 1 Geometric algorithm for binary classification

Input: training data $\mathcal{T}_m = \{(x_i, y_i)\}_{i=1}^m$, iteration number T , stepsize α , parameter k, λ in (5)
Initialize: uniformly sampled grid points $\{\hat{x}_1, \hat{x}_2, \dots, \hat{x}_{d^N}\}$, $f(\hat{x}_j) = \frac{1}{2}$, $\forall j \in \{1, \dots, d^N\}$
for $t = 1$ **to** T **do**
 compute the gradient vector $V_{tot, \lambda, m, f, \phi}(\hat{x}_j)$ for every grid point according to (5) and
 then update the graph by $f(\hat{x}_j) = f(\hat{x}_j) - \alpha V_{tot, \lambda, m, f, \phi}(\hat{x}_j)$
end for

5.2. Experiments

5.2.1. SIMULATIVE EXAMPLE

We first show a simulative example with a $2d$ feature space. As shown in Figure 1, we uniformly sample training data in the square region $[-20, 20] \times [-20, 20]$ in the $2d$ plane, and label points as positive (red) or negative (blue) depending on whether their Euclidean distance from the origin is less than 10. Figure 1 shows the decision boundaries of SVM with RBF kernel and our proposed method after training on these sampled points (both using default parameter settings¹), as well as the graph of our trained function f using the $2d$ grid representation. Note that the decision boundary of our method more closely models the true circle boundary.

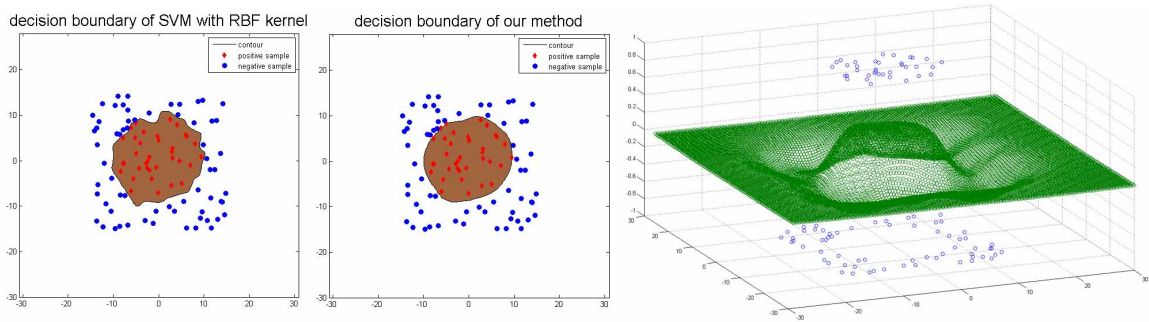


Figure 1: Binary classifier trained on $2d$ data. All training points are sampled uniformly within the region $[-20, 20] \times [-20, 20]$, and labeled by the function $y = \text{sign}(10 - \|\mathbf{x}\|_2)$. The left image shows the decision boundary of SVM with RBF kernel, the middle image shows the decision boundary of our method, and the right image shows the corresponding trained graph of our method.

1. We tried tuning the bandwidth parameter of the RBF kernel. While increasing the bandwidth will lead to a smoother decision boundary, it is very sensitive in that it may also expand the positive region and produce larger training error. In contrast, the decision boundaries of our method are quite robust with respect to parameter settings.

5.2.2. REAL WORLD BENCHMARK

We tested our implementation for binary classification following the setup of [Varshney and Willsky \(2010\)](#), *i.e.*, we report the tenfold cross-validation test error (as a percentage) on four binary classification datasets, as shown in Table 1. On each of the tenfolds, we set the number of iterations T using cross-validation. As with competing methods, in training we perform fivefold cross-validation on the nine tenths of the full dataset which is the training data for that fold. We select the T from the set of values $\{4, 5, 6, 7\}$ that minimizes the fivefold cross-validation test error. We also report our performance (Ours*) without doing cross-validation on T by fixing $T = 5$. Since our current implementation adopts a grid representation of the prediction function f , which requires storing and processing a number of grid points that grows exponentially with the input dimension of feature space, for computational concerns our method first performs PCA to reduce the input feature dimension to 8 for the WDBC and Ionos datasets. Nevertheless, our results (Ours) are overall very strong, attaining top performance on three of the four benchmarks. Even given default parameter settings, our method (Ours*) still attains top three performances on all datasets, showing the robustness of our method to hyper-parameter settings.

Table 1: Ten-fold cross-validation error rate (percent) on four binary classification datasets from the UCI machine learning repository. d denotes the input feature dimension. We compare our method (Ours) and a fixed T parameter version (Ours*) with 10 methods reported in Table 1 of [Varshney and Willsky \(2010\)](#): Naïve Bayes (NB), Bayes net classifier (BN), k -nearest neighbor with inverse distance weighting (kNN), C4.4 decision tree (C4.4), C4.5 decision tree (C4.5), Naïve Bayes tree classifier (NBT), SVM with polynomial kernel (SVM), Radial basis function network (RBN), Level learning set classifier ([Cai and Sowmya, 2007](#)) (LLS), Geometric level set classifier ([Varshney and Willsky, 2010](#)) (GLS). Top performance for each dataset is highlighted in bold.

DATASET(d)	NB	BN	kNN	C4.4	C4.5	NBT	SVM	RBN	LLS	GLS	OURS	OURS*
PIMA(8)	23.69	25.64	27.86	27.33	26.17	25.64	22.66	24.60	29.94	25.94	22.52	22.91
WDBC(30)	7.02	4.92	3.68	7.20	6.85	7.21	2.28	5.79	6.50	4.40	3.34	3.34
LIVER(6)	44.61	43.75	41.75	31.01	31.29	33.87	41.72	35.65	37.39	37.61	30.95	31.24
IONOS.(34)	17.38	10.54	17.38	8.54	8.54	10.27	11.40	7.38	13.11	13.67	6.76	7.59

6. Discussion

We have proposed a differential geometric approach to classification. There are several directions for future research. In the theoretical direction, the rate of convergence of the algorithm should be studied, particularly in light of our idea of controlling the oscillatory nature of the conditional label probability. For practical applications, we intend to implement the extension to the multi-class classification problem (Theorem 2). It is also interesting to investigate possible parametric representations of f which would enable closed-form computation of derivatives of f and as a result, the most informative measure of curvature (Theorem 1) could be adopted in practice. Finally, these geometric methods have natural extensions to more general manifold learning problems with more informative regularization terms; indeed, although there are at present numerical and memory obstacles to implementation, the theoretical extension is in place (see Theorem 1).

References

- Jean-Yves Audibert and Alexandre Tsybakov. Fast learning rates for plug-in classifiers. *Annals of Statistics*, 35(2):608–633, 2007.
- Michèle Audin and Mihai Damian. *Morse Theory and Floer Homology*. Universitext. Springer, London; EDP Sciences, Les Ulis, 2014.
- Qinxun Bai, Dara Gold, and Steven Rosenberg. In preperation, 2015.
- Mikhail Belkin and Partha Niyogi. Laplacian eigenmaps for dimensionality reduction and data representation. *Neural Computation*, 15(6):1373–1396, 2003.
- Olivier Bousquet and André Elisseeff. Stability and generalization. *Journal of Machine Learning Research*, 2:499–526, 2002.
- Xiongcai Cai and Arcot Sowmya. Level learning set: A novel classifier based on active contour models. In *Proc. European Conf. on Machine Learning (ECML)*, pages 79–90. 2007.
- Yun-Gang Chen, Yoshikazu Giga, and Shun’ichi Goto. Uniqueness and existence of viscosity solutions of generalized mean curvature flow equations. In *Fundamental contributions to the continuum theory of evolving phase interfaces in solids*, pages 375–412. Springer, Berlin, 1999.
- Thomas Cover and Peter Hart. Nearest neighbor pattern classification. *IEEE Trans. Information Theory*, 13(1):21–27, 1967.
- Luc Devroye, László Györfi, and Gábor Lugosi. *A probabilistic theory of pattern recognition*. Springer, 1996.
- David Donoho and Carrie Grimes. Hessian eigenmaps: Locally linear embedding techniques for high-dimensional data. *Proceedings of the National Academy of Sciences*, 100(10):5591–5596, 2003.
- Arnaud Gelas, Olivier Bernard, Denis Friboulet, and Rémy Prost. Compactly supported radial basis functions based collocation method for level-set evolution in image segmentation. *Image Processing, IEEE Transactions on*, 16(7):1873–1887, 2007.
- John Guckenheimer and Patrick Worfolk. Dynamical systems: some computational problems. In *Bifurcations and periodic orbits of vector fields (Montreal, PQ, 1992)*, volume 408 of *NATO Adv. Sci. Inst. Ser. C Math. Phys. Sci.*, pages 241–277. Kluwer Acad. Publ., Dordrecht, 1993.
- Richard Hamilton. The inverse function theorem of Nash and Moser. *Bull. Amer. Math. Soc. (N.S.)*, 7:65–222, 1982.
- William Jagy. Minimal hypersurfaces foliated by spheres. *Michigan Math. J.*, 38:255–270, 1991.
- H. Blaine Lawson, Jr. *Lectures on minimal submanifolds. Vol. I*, volume 9 of *Mathematics Lecture Series*. Publish or Perish, Inc., Wilmington, Del., second edition, 1980.
- Tong Lin and Hongbin Zha. Riemannian manifold learning. *Pattern Analysis and Machine Intelligence, IEEE Transactions on*, 30(5):796–809, 2008.

- Tong Lin, Hanlin Xue, Ling Wang, and Hongbin Zha. Total variation and Euler’s elastica for supervised learning. *Proc. International Conf. on Machine Learning (ICML)*, 2012.
- Carlo Mantegazza. *Lecture Notes on Mean Curvature Flow*, volume 290 of *Progress in Mathematics*. Birkhäuser/Springer Basel AG, Basel, 2011.
- John Milnor. *Morse Theory*. Annals of Mathematics Studies, No. 51. Princeton University Press, Princeton, N.J., 1963.
- Stanley Osher and James Sethian. Fronts propagating with curvature-dependent speed: algorithms based on hamilton-jacobi formulations. *Journal of Computational Physics*, 79(1):12–49, 1988.
- Sam Roweis and Lawrence Saul. Nonlinear dimensionality reduction by locally linear embedding. *Science*, 290(5500):2323–2326, 2000.
- Bernhard Schölkopf and year=2002 publisher=MIT press Smola, Alexander. *Learning with kernels: Support vector machines, regularization, optimization, and beyond*.
- Ingo Steinwart. Consistency of support vector machines and other regularized kernel classifiers. *IEEE Trans. Information Theory*, 51(1):128–142, 2005.
- Charles Stone. Consistent nonparametric regression. *Annals of Statistics*, pages 595–620, 1977.
- Joshua Tenenbaum, Vin De Silva, and John Langford. A global geometric framework for nonlinear dimensionality reduction. *Science*, 290(5500):2319–2323, 2000.
- Vladimir Naumovich Vapnik. *Statistical learning theory*, volume 1. Wiley New York, 1998.
- Kush Varshney and Alan Willsky. Classification using geometric level sets. *Journal of Machine Learning Research*, 11:491–516, 2010.
- Zhenyue Zhang and Hongyuan Zha. Principal manifolds and nonlinear dimensionality reduction via tangent space alignment. *SIAM Journal on Scientific Computing*, 26(1):313–338, 2005.

Appendix A. Notation

Probability notation:

$$\begin{aligned}
 \mathcal{X} \subset \mathbb{R}^N & : \text{input feature space} \\
 \mathcal{Y} = \{1, -1\} & : \text{label space} \\
 P(X, Y) \sim \mathcal{X} \times \mathcal{Y} & : \text{underlying distribution that generates the data and its label} \\
 \mu(\mathbf{x}) & : \text{marginal distribution of } \mathbf{x} \\
 \eta(\mathbf{x}) = P(y = 1|\mathbf{x}) & : \text{conditional label probability} \\
 \mathcal{T}_m = \{(\mathbf{x}_i, y_i)\}_{i=1}^m \in (\mathcal{X} \times \mathcal{Y})^m & : \text{training set} \\
 \text{sign}(x) & = \begin{cases} 1, & x \geq 0, \\ -1, & \text{otherwise.} \end{cases} \\
 \mathbb{1}_{\text{sign}(f(\mathbf{x})-0.5) \neq y} & = \begin{cases} 1, & \text{sign}(f(\mathbf{x}) - 0.5) \neq y, \\ 0, & \text{sign}(f(\mathbf{x}) - 0.5) = y. \end{cases} \\
 R_P(f) = \mathbb{E}_P[\mathbb{1}_{\text{sign}(f(\mathbf{x})-0.5) \neq y}] & : \text{generalization risk for the estimator } f : \mathcal{X} \rightarrow [0, 1] \\
 R_P^* = \inf_{f: \mathcal{X} \rightarrow \mathbb{R}} R_P(f) & : \text{Bayes risk} \\
 (D\text{-risk for our } \mathcal{P}_D) R_{D,P}(f) & = \int_{\mathcal{X}} d^2(f(\mathbf{x}), \eta(\mathbf{x})) dx \\
 (\text{empirical } D\text{-risk}) R_{D,\mathcal{T}_m}(f) = R_{D,\mathcal{T}_m,k}(f) & = \int_{\mathcal{X}} d^2 \left(f(\mathbf{x}), \frac{1}{k} \sum_i^k \tilde{x}_i^{N+1} \right) dx, \\
 & \text{where } \tilde{x}_i^{N+1} \in \{0, 1\} \text{ is the } (N+1)\text{-st component value} \\
 & \text{associated to the } i\text{-th nearest neighbor in } \mathcal{T}_m \text{ to } \mathbf{x} \\
 R_{D,P,\lambda}^\Omega(f) = R_{D,P}(f) + \lambda \Omega(f) & : \text{regularized } D\text{-risk for the function } f \\
 R_{D,\mathcal{T}_m,\lambda}^\Omega(f) = R_{D,\mathcal{T}_m}(f) + \lambda \Omega(f) & : \text{regularized empirical } D\text{-risk for the function } f \\
 f_{D,P,\lambda} & = \text{function attaining the global minimum for } R_{D,P,\lambda}^\Omega \\
 R_{D,P,\lambda}^* = R_{D,P,\lambda}^\Omega(f_{D,P,\lambda}) & : \text{minimum value for } R_{D,P,\lambda}^\Omega \\
 f_{D,\mathcal{T}_m,\lambda} = f_{D,\mathcal{T}_m,k,\lambda} & : \text{function attaining the global minimum for } R_{D,\mathcal{T}_m,\lambda}^\Omega(f)
 \end{aligned}$$

Note that we assume $f_{D,P,\lambda}$ and $f_{D,\mathcal{T}_m,\lambda}$ exist.

Geometry notation:

$\text{Maps}(\mathcal{X}, \mathbb{R})$:	$\{f : \mathcal{X} \rightarrow \mathbb{R} : f \in C^\infty\}$
\mathcal{M}	:	$\{f : \mathcal{X} \rightarrow (-\epsilon, 1 + \epsilon) : f \in C^\infty\}$ for a fixed small $\epsilon > 0$
$T_f \mathcal{M}$:	the tangent space to \mathcal{M} at some $f \in \mathcal{M}$; $T_f \mathcal{M} \simeq \text{Maps}(\mathcal{X}, \mathbb{R})$
The graph of $f \in \text{Maps}(\mathcal{X}, \mathbb{R})$:	$\text{gr}(f) = \{(x, f(x)) : x \in \mathcal{X}\}$
$g_{ij} = \frac{\partial f}{\partial x^i} \frac{\partial f}{\partial x^j}$:	The Riemannian metric on the graph of f induced from the standard dot product on \mathbb{R}^{N+1}
(g^{ij})	=	g^{-1} , with $g = (g_{ij})_{i,j=1,\dots,N}$
$\text{dvol}_x = \text{dvol}_{\text{gr}(f)}$	=	$\sqrt{\det(g)} dx^1 \dots dx^N$, the volume element on $\text{gr}(f)$
$\{e_i\}_{i=1}^N$:	a smoothly varying orthonormal basis of the tangent spaces $T_{(x,f(x))\text{gr}(f)}$ of the graph of f
Tr II	:	the trace of the second fundamental form, Tr II
	=	$\left(\sum_{i=1}^N D_{e_i} e_i \right) \cdot \nu$, with ν the unit upward normal to the graph of f , and $D_y w$ the directional derivative of w in the direction y
∇P	:	the gradient vector field of a function $P : A \rightarrow \mathbb{R}$ on a possibly infinite dimensional manifold A
$\mathcal{R} = \mathcal{R}_f$:	the Riemannian curvature of the graph of f

\mathcal{R} is a four-tensor, with components $R_{sjkl} = g_{si} R^i_{jkl}$, with

$$R^i_{jkl} = \frac{\partial \Gamma^i_{jk}}{\partial x^l} - \frac{\partial \Gamma^i_{jl}}{\partial x^k} + \Gamma^t_{jk} \Gamma^i_{tl} - \Gamma^t_{jl} \Gamma^i_{tk}, \text{ with } \Gamma^i_{jk} = \frac{1}{2} g^{il} \left(\frac{\partial g_{kl}}{\partial x^j} + \frac{\partial g_{jl}}{\partial x^k} - \frac{\partial g_{jk}}{\partial x^l} \right),$$

with summation convention.

Appendix B. Proofs of the Steps for Theorem 3

B.1. Step 1

Lemma 4 (Step 1) $\lim_{\lambda \rightarrow 0} R^*_{D,P,\lambda} = 0$.

Proof After the smoothing procedure in §3.1 for the distance penalty term, the function $R^{\Omega}_{D,P,\lambda} : \text{Maps}(\mathcal{X}, [0, 1]) \rightarrow \mathbb{R}$ is continuous in the Fréchet topology on $\text{Maps}(\mathcal{X}, [0, 1])$, the space of smooth maps from \mathcal{X} to $[0, 1]$. We check that the functions $R^{\Omega}_{D,P,\lambda} : \text{Maps}(\mathcal{X}, [0, 1]) \rightarrow \mathbb{R}$ are equicontinuous in λ : for fixed $f_0 \in \text{Maps}(\mathcal{X}, [0, 1])$ and $\epsilon > 0$, there exists $\delta = \delta(f_0, \epsilon)$ such that $|\lambda - \lambda'| < \delta \Rightarrow |R^{\Omega}_{D,P,\lambda}(f_0) - R^{\Omega}_{D,P,\lambda'}(f_0)| < \epsilon$. This is immediate:

$$|R^{\Omega}_{D,P,\lambda}(f_0) - R^{\Omega}_{D,P,\lambda'}(f_0)| = |(\lambda - \lambda') \Omega(f_0)| < \epsilon,$$

if $\delta < \epsilon/|\Omega(f_0)|$. It is standard that the infimum $\inf R_{\lambda}$ of an equicontinuous family of functions is continuous in λ , so $\lim_{\lambda \rightarrow 0} R^*_{D,P,\lambda} = R^*_{D,P,\lambda=0} = R_{D,P}(\eta) = 0$. \blacksquare

B.2. Step 2

We assume that the conditional label probability $\eta(\mathbf{x}) : \mathbb{R}^N \rightarrow \mathbb{R}$ is smooth, and that the marginal distribution $\mu(\mathbf{x})$ is continuous.

Notation: (1)

$$\widetilde{\text{sign}}(x) = \text{sign}(x - .05) = \begin{cases} 1, & x \geq 0.5, \\ -1, & x < .05. \end{cases}$$

Thus

$$\mathbb{1}_{\text{sign}(f(\mathbf{x}) - 0.5) \neq y} = \begin{cases} 1, & \widetilde{\text{sign}}(f(\mathbf{x})) \neq y, \\ 0, & \widetilde{\text{sign}}(f(\mathbf{x})) = y. \end{cases}$$

(2) Let $\mathcal{X}_{1,f} = \{\mathbf{x} \in \mathcal{X} : f(\mathbf{x}) \geq 0.5\}$, $\mathcal{X}_{2,f} = \{\mathbf{x} \in \mathcal{X} : f(\mathbf{x}) < 0.5\}$, let $\mathcal{X}_1, \mathcal{X}_2$ be the corresponding sets for η , and let $\mathcal{X}_{1,n} = \mathcal{X}_{1,f_n}$, $\mathcal{X}_{2,n} = \mathcal{X}_{2,f_n}$.

(3) The measure μ on \mathcal{X} is defined by $\mu(A) = \int_A \mu(\mathbf{x}) d\mathbf{x}$.

Then

$$\begin{aligned} \mathbb{E}_P[\mathbb{1}_{\text{sign}(f(\mathbf{x}) - 0.5) \neq y}] &= \int_{\mathcal{X}} [\mathbb{1}_{\widetilde{\text{sign}}(f(\mathbf{x})) \neq 1} + p(y = -1 | \mathbf{x}) \mathbb{1}_{\widetilde{\text{sign}}(f(\mathbf{x})) \neq -1}] \mu(\mathbf{x}) d\mathbf{x} \\ &= \int_{\mathcal{X}_{1,f}} (1 - p(y = -1 | \mathbf{x})) \mu(\mathbf{x}) d\mathbf{x} + \int_{\mathcal{X}_{2,f}} p(y = -1 | \mathbf{x}) \mu(\mathbf{x}) d\mathbf{x}. \end{aligned}$$

Thus

$$\mathbb{E}_P[\mathbb{1}_{\text{sign}(f(\mathbf{x}) - 0.5) \neq y}] = \mathbb{E}_P[\mathbb{1}_{\widetilde{\text{sign}}(f(\mathbf{x})) \neq y}] = \int_{\mathcal{X}} [\delta_{1, \widetilde{\text{sign}}(f)} - \widetilde{\text{sign}}(f)] \mu(\mathbf{x}) d\mathbf{x}.$$

Lemma 5 (Step 2 for a subsequence)

$$\lim_{n \rightarrow \infty} R_{D,P}(f_n) = 0 \Rightarrow \lim_{i \rightarrow \infty} R_P(f_{n_i}) = R_P^*$$

for some subsequence $\{f_{n_i}\}_{i=1}^{\infty}$ of $\{f_n\}$.

Proof The left hand terms in the Lemma become

$$\int_{\mathcal{X}} d_{\mathbb{R}^2}^2((\mathbf{x}, f_n(\mathbf{x})), (\mathbf{x}, \eta(\mathbf{x}))) d\mathbf{x} = \int_{\mathcal{X}} d_{\mathbb{R}}^2(f_n(\mathbf{x}), \eta(\mathbf{x})) \mu(\mathbf{x}) d\mathbf{x} \rightarrow 0, \quad (9)$$

so it suffices to show

$$\begin{aligned} \int_{\mathcal{X}} d^2(f_n(\mathbf{x}), \eta(\mathbf{x})) \mu(\mathbf{x}) d\mathbf{x} &\rightarrow 0 \\ \implies \mathbb{E}_P[\mathbb{1}_{\widetilde{\text{sign}}(f(\mathbf{x})) \neq y}] &\rightarrow \mathbb{E}_P[\mathbb{1}_{\widetilde{\text{sign}}(\eta(\mathbf{x})) \neq y}]. \end{aligned} \quad (10)$$

We recall that L^2 convergence implies pointwise convergence a.e, so (9) implies that a subsequence of f_n , also denoted f_n , has $f_n \rightarrow \eta(\mathbf{x})$ pointwise a.e. on \mathcal{X} . (By our assumption on $\mu(\mathbf{x})$, these statements hold for either μ or Lebesgue measure.) Egorov's theorem implies that for any $\epsilon > 0$, there exists a set $B_\epsilon \subset \mathcal{X}$ with $\mu(B_\epsilon) < \epsilon$ such that $f_n \rightarrow \eta(\mathbf{x})$ uniformly on $\mathcal{X} \setminus B_\epsilon$.

Fix $\delta > 0$ and set $Z_\delta = \{\mathbf{x} \in \mathcal{X} : |\eta(\mathbf{x}) - 0.5| < \delta\}$. For the moment, assume that $Z_0 = \{\mathbf{x} \in \mathcal{X} : \eta(\mathbf{x}) = 0.5\}$ has $\mu(Z_0) = 0$. It follows easily² that $\mu(Z_\delta) \rightarrow 0$ as $\delta \rightarrow 0$. On $\mathcal{X} \setminus (Z_\delta \cup B_\epsilon)$, we have $\mathbb{1}_{\widetilde{\text{sign}(f_n(\mathbf{x})) \neq y}} = \mathbb{1}_{\widetilde{\text{sign}(\eta(\mathbf{x})) \neq y}}$ for $n > N_\delta$. Thus

$$\mathbb{E}_P[\mathbb{1}_{\mathcal{X} \setminus (Z_\delta \cup B_\epsilon)} \mathbb{1}_{\widetilde{\text{sign}(f_n(\mathbf{x})) \neq y}}] = \mathbb{E}_P[\mathbb{1}_{\mathcal{X} \setminus (Z_\delta \cup B_\epsilon)} \mathbb{1}_{\widetilde{\text{sign}(\eta(\mathbf{x})) \neq y}}].$$

(Here $\mathbb{1}_A$ is the characteristic function of a set A .)

As $\delta \rightarrow 0$,

$$\mathbb{E}_P[\mathbb{1}_{\mathcal{X} \setminus (Z_\delta \cup B_\epsilon)} \mathbb{1}_{\widetilde{\text{sign}(f_n(\mathbf{x})) \neq y}}] \rightarrow \mathbb{E}_P[\mathbb{1}_{\mathcal{X} \setminus B_\epsilon} \mathbb{1}_{\widetilde{\text{sign}(f_n(\mathbf{x})) \neq y}}].$$

and similarly for f_n replaced by $\eta(\mathbf{x})$. During this process, N_δ presumably goes to ∞ , but that precisely means

$$\lim_{n \rightarrow \infty} \mathbb{E}_P[\mathbb{1}_{\mathcal{X} \setminus B_\epsilon} \mathbb{1}_{\widetilde{\text{sign}(f_n(\mathbf{x})) \neq y}}] = \mathbb{E}_P[\mathbb{1}_{\mathcal{X} \setminus B_\epsilon} \mathbb{1}_{\widetilde{\text{sign}(\eta(\mathbf{x})) \neq y}}].$$

Since

$$\left| \mathbb{E}_P[\mathbb{1}_{\mathcal{X} \setminus B_\epsilon} \mathbb{1}_{\widetilde{\text{sign}(f_n(\mathbf{x})) \neq y}}] - \mathbb{E}_P[\mathbb{1}_{\widetilde{\text{sign}(f_n(\mathbf{x})) \neq y}}] \right| < \epsilon,$$

and similarly for $\eta(\mathbf{x})$, we get

$$\begin{aligned} & \left| \lim_{n \rightarrow \infty} \mathbb{E}_P[\mathbb{1}_{\widetilde{\text{sign}(f_n(\mathbf{x})) \neq y}}] - \mathbb{E}_P[\mathbb{1}_{\widetilde{\text{sign}(\eta(\mathbf{x})) \neq y}}] \right| \\ & \leq \left| \lim_{n \rightarrow \infty} \mathbb{E}_P[\mathbb{1}_{\widetilde{\text{sign}(f_n(\mathbf{x})) \neq y}}] - \lim_{n \rightarrow \infty} \mathbb{E}_P[\mathbb{1}_{\mathcal{X} \setminus B_\epsilon} \mathbb{1}_{\widetilde{\text{sign}(f_n(\mathbf{x})) \neq y}}] \right| \\ & \quad + \left| \lim_{n \rightarrow \infty} \mathbb{E}_P[\mathbb{1}_{\mathcal{X} \setminus B_\epsilon} \mathbb{1}_{\widetilde{\text{sign}(f_n(\mathbf{x})) \neq y}}] - \mathbb{E}_P[\mathbb{1}_{\mathcal{X} \setminus B_\epsilon} \mathbb{1}_{\widetilde{\text{sign}(\eta(\mathbf{x})) \neq y}}] \right| \\ & \quad + \left| \lim_{n \rightarrow \infty} \mathbb{E}_P[\mathbb{1}_{\mathcal{X} \setminus B_\epsilon} \mathbb{1}_{\widetilde{\text{sign}(\eta(\mathbf{x})) \neq y}}] - \mathbb{E}_P[\mathbb{1}_{\widetilde{\text{sign}(\eta(\mathbf{x})) \neq y}}] \right| \\ & \leq 3\epsilon. \end{aligned}$$

(Strictly speaking, $\lim_{n \rightarrow \infty} \mathbb{E}_P[\mathbb{1}_{\widetilde{\text{sign}(f_n(\mathbf{x})) \neq y}}]$ is first lim sup and then lim inf to show that the limit exists.) Since ϵ is arbitrary, the proof is complete if $\mu(Z_0) = 0$.

If $\mu(Z_0) > 0$, we rerun the proof with \mathcal{X} replaced by Z_0 . As above, $f_n|_{Z_0}$ converges uniformly to $\eta(\mathbf{x})$ off a set of measure ϵ . The argument above, without the set Z_δ , gives

$$\int_{Z_0} \mathbb{1}_{\text{sign}(f_n(\mathbf{x}) - 0.5) \neq y} \mu(\mathbf{x}) d\mathbf{x} \rightarrow \int_{Z_0} \mathbb{1}_{\text{sign}(-0.5) \neq y} \mu(\mathbf{x}) d\mathbf{x}.$$

We then proceed with the proof above on $\mathcal{X} \setminus Z_0$. ■

Corollary 6 (Step 2 in general) For our algorithm, $\lim_{n \rightarrow \infty} R_{D,P}(f_{n,\lambda,m}) = 0 \Rightarrow \lim_{i \rightarrow \infty} R_P(f_{n,\lambda,m}) = R_P^*$.

2. Let A_k be sets with $A_{k+1} \subset A_k$ and with $\mu(\cap_{k=1}^\infty A_k) = 0$. If $\mu(A_k) \not\rightarrow 0$, then there exists a subsequence, also called A_k , with $\mu(A_k) > K > 0$ for some K . We claim $\mu(\cap A_k) \geq K$, a contradiction. For the claim, let $Z = \cap A_k$. If $\mu(Z) \geq \mu(A_k)$ for all k , we are done. If not, since the A_k are nested, we can replace A_k by a set, also called A_k , of measure K and such that the new A_k are still nested. For the relabeled $Z = \cap A_k$, $Z \subset A_k$ for all k , and we may assume $\mu(Z) < K$. Thus there exists $Z' \subset A_1$ with $Z' \cap Z = \emptyset$ and $\mu(Z') > 0$. Since $\mu(A_i) = K$, we must have $A_i \cap Z' \neq \emptyset$ for all i . Thus $\cap A_i$ is strictly larger than Z , a contradiction. In summary, the claim must hold, so we get a contradiction to assuming $\mu(A_k) \not\rightarrow 0$.

Proof Choose $f_{1,\lambda,m}$ as in Theorem 3. Since $V_{tot,\lambda,m,f_{n,\lambda,m}}$ has pointwise length going to zero as $n \rightarrow \infty$, $\{f_{n,\lambda,m}(\mathbf{x})\}$ is a Cauchy sequence for all \mathbf{x} . This implies that $f_{n,\lambda,m}$, and not just a subsequence, converges pointwise to η . \blacksquare

B.3. Step 3

Lemma 7 (Step 3) *If $k \rightarrow \infty$ and $k/m \rightarrow 0$ as $m \rightarrow \infty$, then for $f \in \text{Maps}(\mathcal{X}, [0, 1])$,*

$$|R_{D,\mathcal{T}_m}(f) - R_{D,P}(f)| \xrightarrow{m \rightarrow \infty} 0,$$

for all distributions p .

Proof We have

$$\begin{aligned} |R_{D,\mathcal{T}_m}(f) - R_{D,P}(f)| &= \left| \int_{\mathcal{X}} \left[d^2 \left(f(\mathbf{x}), \frac{1}{k} \sum_i^k \tilde{x}_i^{N+1} \right) - d^2(f(\mathbf{x}), \eta(\mathbf{x})) \right] \mu(\mathbf{x}) d\mathbf{x} \right| \\ &\leq \int_{\mathcal{X}} \left| d^2 \left(f(\mathbf{x}), \frac{1}{k} \sum_i^k \tilde{x}_i^{N+1} \right) - d^2(f(\mathbf{x}), \eta(\mathbf{x})) \right| \mu(\mathbf{x}) d\mathbf{x}. \end{aligned}$$

Set $a = d^2 \left(f(\mathbf{x}), \frac{1}{k} \sum_i^k \tilde{x}_i^{N+1} \right)$, $b = d^2(f(\mathbf{x}), \eta(\mathbf{x}))$. Then $|a^2 - b^2| \leq 2|a - b| \max\{|a|, |b|\} \leq 2|a - b|$, since $f(\mathbf{x}), \frac{1}{k} \sum_i^k \tilde{x}_i^{N+1}, \eta(\mathbf{x}) \in [0, 1]$. Also, $\int_{\mathcal{X}} |a - b| \mu(\mathbf{x}) d\mathbf{x} \leq \text{vol}(\mathcal{X}) \int_{\mathcal{X}} |a - b|^2 \mu(\mathbf{x}) d\mathbf{x}$ by Cauchy-Schwarz. Therefore, it suffices to show that

$$\int_{\mathcal{X}} \left| d \left(f(\mathbf{x}), \frac{1}{k} \sum_i^k \tilde{x}_i^{N+1} \right) - d(f(\mathbf{x}), \eta(\mathbf{x})) \right|^2 \mu(\mathbf{x}) d\mathbf{x} \xrightarrow{m \rightarrow \infty} 0.$$

Since $|d(f(\mathbf{x}), \frac{1}{k} \sum_i^k \tilde{x}_i^{N+1}) - d(f(\mathbf{x}), \eta(\mathbf{x}))| \leq |\eta(\mathbf{x}) - \frac{1}{k} \sum_i^k \tilde{x}_i^{N+1}|$, the result follows if

$$\lim_{m \rightarrow \infty} \mathbb{E}_P \left[\left(\eta(\mathbf{x}) - \frac{1}{k} \sum_i^k \tilde{x}_i^{N+1} \right)^2 \right] = 0. \quad (11)$$

For $\eta_m(\mathbf{x}) = \frac{1}{k} \sum_i^k \tilde{x}_i^{N+1}$, η_m is actually an estimate of the conditional label probability $\eta(\mathbf{x})$ by the k -Nearest Neighbor rule. According to Stone's Theorem (Stone, 1977; Devroye et al., 1996), if $k \xrightarrow{m \rightarrow \infty} \infty$ and $k/m \xrightarrow{m \rightarrow \infty} 0$, (11) holds for all distributions P . \blacksquare

Appendix C. Implementation Details

For classification experiments with the trained f , we need to evaluate $f(\mathbf{x})$ for all $\mathbf{x} \in \mathcal{X}$, not just at grid points. We use standard linear interpolation techniques (such as those provided in Matlab). The final predictor is given by

$$F(\mathbf{x}) = \begin{cases} 1, & f(\mathbf{x}) \geq 0.5, \\ -1, & f(\mathbf{x}) < 0.5. \end{cases} \quad (12)$$

In our current implementation, we further simplify the distance vector field (2) by choosing $k = 1$ and replacing $\phi(\mathbf{x})$ by a simple function to get the following formula:

$$V_{D,f}(\mathbf{x}) = \frac{(\mathbf{0}, f(\mathbf{x}) - \tilde{x}_1^{N+1})}{\|\mathbf{x} - \tilde{\mathbf{x}}_1\|}, \quad (13)$$

Then the total vector field is

$$\begin{aligned} V_{tot,\lambda,m,f} &= V_{D,f} + \lambda V_{G,f} \\ &= \frac{(\mathbf{0}, f(\mathbf{x}) - \tilde{x}_1^{N+1})}{\|\mathbf{x} - \tilde{\mathbf{x}}_1\|} + \lambda(\text{Tr } \Pi \cdot e_{N+1})e_{N+1}, \end{aligned} \quad (14)$$

The algorithm is the same as Algorithm 1, with (5) just replaced with (14). We then have three hyper-parameters we need to specify: the iteration number T , the stepsize α , and the trade-off parameter λ in (14). In practice, we could further simplify the algorithm to reduce the number of hyper-parameters. The intuition is that given the initial graph is a hyperplane, in step 1 of Algorithm 1, the geometric penalty is zero and $V_{tot,\lambda,m,f} = V_{D,f}$. Actually, after step 1, according to (13), the resulting predictor (12) already makes no error on the training set. In other words, the graph of f is already overfitted to the training data. So in later steps, we could apply the geometric gradient only to “smooth” the graph of f , to obtain a trade-off between fitting the training data and keeping the graph as flat as possible. While this simplification might lose the theoretical guarantee of Bayes consistency, we found it to work essentially as well as Algorithm 1 in our experiments but much faster. In addition, the number of hyper-parameters is reduced to two: the iteration number T and the stepsize α . As a result, we adopt this simplified version in our real world benchmark experiments reported in §5.2.2, where we always set $\alpha = 0.1$, and fix T (Ours*) or do cross-validation on training data to select T (Ours). This simplified version of the algorithm is summarized in Algorithm 2.

Algorithm 2 Geometric algorithm for binary classification (simplified)

Input: training data $\mathcal{T}_m = \{(\mathbf{x}_i, y_i)\}_{i=1}^m$, iteration number T , stepsize α
Initialize: uniformly sampled grid points $\{\hat{\mathbf{x}}_1, \hat{\mathbf{x}}_2, \dots, \hat{\mathbf{x}}_{d^N}\}$, $f(\hat{\mathbf{x}}_j) = \frac{1}{2}$, $\forall j \in \{1, \dots, d^N\}$
 compute the distance gradient vector $V_{D,f}(\hat{\mathbf{x}}_j)$ for every grid point according to (13) and then update the graph by $f(\hat{\mathbf{x}}_j) = f(\hat{\mathbf{x}}_j) - V_{D,f}(\hat{\mathbf{x}}_j)$
for $t = 1$ **to** T **do**
 compute the geometric gradient vector $V_{G,f}(\hat{\mathbf{x}}_j)$ for every grid point according to (4)
 and then update the graph by $f(\hat{\mathbf{x}}_j) = f(\hat{\mathbf{x}}_j) - \alpha V_{G,f}(\hat{\mathbf{x}}_j)$
end for
